

Quantum metrology with quantum Wheatstone bridge composed of Bose systems

Dong Xie,^{1,*} Chunling Xu,^{1,†} Xiwei Yao,¹ and An Min Wang²

¹*School of Science, Guilin University of Aerospace Technology,
Guilin, Guangxi 541004, People's Republic of China*

²*Department of Modern Physics, University of Science and Technology of China,
Hefei, Anhui 230026, People's Republic of China*

The quantum version of a special classical Wheatstone bridge built with a boundary-driven spin system has recently been proposed. We propose a quantum Wheatstone bridge consisting of Bose systems, which can simulate the general classical Wheatstone bridge. Unknown coupling can be obtained when the quantum Wheatstone bridge is balanced, which can be determined simply by the homodyne detection. When the expectation value of the homodyne detection is 0, the quantum Wheatstone bridge is unbalanced. Regulate a known coupling strength to make the expectation value of the homodyne detection be proportional to the square root of the initial number of bosons, which means that the quantum Wheatstone bridge is balanced. By calculating the quantum Fisher information, we show that the measurement precision is optimal when the quantum Wheatstone bridge is balanced. And the homodyne detection is close to the optimal measurement in the case of low-temperature baths.

I. INTRODUCTION

The classical Wheatstone bridge is an instrument for accurate measurement of electrical resistance. Although its structure is simple, its accuracy and sensitivity are relatively high, and it has been widely used in medical diagnosis, testing instruments and automatic centering control [1–3]. It was invented by English inventor Christie in 1833 [4], but it became known because Wheatstone [5] was the first to use it to measure resistance. As shown in Fig. 1, there are three known and tunable resistances (R_1 , R_2 , R_3), and the Resistance R_x to be measured. By varying the three tunable resistances until the indicator of galvanometer A is 0, the classical Wheatstone bridge is in balance. At the balance point, the value of R_x can be obtained

$$R_x = \frac{R_2}{R_1} R_3. \quad (1)$$

With the study of smaller and smaller scale, quantum effects are gradually prominent. Based on the quantum estimation theory [6], there are many works exploring the use of quantum resources to improve parameter measurement precision, such as, quantum magnetometer [7–9], quantum thermometry [10–15], quantum interferometry [16], and Quantum illumination [17–19].

Recently, Poulsen *et al.* [20] utilized a few-body boundary-driven spin chain to build a quantum version of the special Wheatstone bridge with $R_1 = R_2$. In this article, we propose a quantum Wheatstone bridge consisting of Bose systems, which can simulate the general classical Wheatstone bridge, as shown in Fig. 2. Similar to the classical Wheatstone bridge, the unknown coupling

strength J_x in the quantum Wheatstone bridge composed of Bose systems can be obtained at the balance point

$$J_x = \frac{J_2}{J_1} J_3. \quad (2)$$

In Ref. [20], they only considered the case of $J_2 = J_1$. And they got the unknown strength at the balance point by the formula $J_x = \lambda J_3$, where the coefficient λ was not equal to 1. It deviates from the classical Wheatstone bridge and is therefore not a strictly quantum Wheatstone bridge.

In this article, we are able to simply judge the bridge balance by the local homodyne detection of cavity mode 2 or 3. When $J_1 = J_2$, the quantum Wheatstone bridge can be further simplified with $J_0 = 0$. By analytically calculating the quantum Fisher information, we show that the homodyne detection is close to the optimal measurement in the case of low-temperature baths. The quantum fluctuation from the thermal baths will reduce the measurement precision. With the optimal measurement, measurement precision becomes more and more independent with the increase of fluctuation intensity. For resisting the dissipation of cavity modes 2 and 3, the gain process is proposed to maintain the criteria for quantum Wheatstone bridge balance.

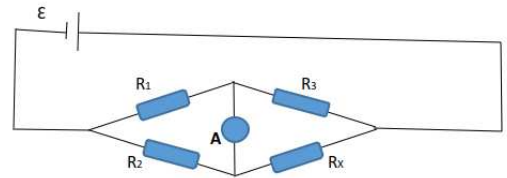


Figure 1. Schematic diagram of the classical Wheatstone bridge. It is composed of three controllable resistances (R_1 , R_2 , R_3), and the Resistance R_x to be measured. A denotes a galvanometer.

* xiedong@mail.ustc.edu.cn

† xuchunling@guat.edu.cn

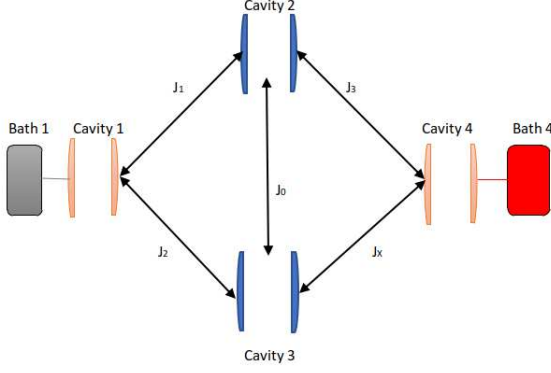


Figure 2. Schematic diagram of the quantum Wheatstone bridge. This bridge is composed of 4 cavity modes. There are four tunable and known coupling strengths J_1 , J_2 , J_3 , J_0 and one coupling strength J_x to be measured. Cavity modes 1 and 4 are interacting with two thermal baths with temperature T_1 and T_4 .

This article is organized as follows. In Section II, we introduce the setup of the quantum Wheatstone bridge. In section III, the balance criterion of quantum Wheatstone bridge is given. The measurement precision with the homodyne detection is achieved in section IV. By calculating the quantum Fisher information, the optimal precision is obtained in section V. We propose a way to deal with the extra dissipation in section VI. The experiment feasibility of our scheme is discussed in section VII. Finally, we make a simple conclusion in section VIII.

II. SETUP CONSISTING OF THE CAVITY MODES

We propose to build the quantum Wheatstone bridge composed of Bose systems, taking the cavity modes as an example, as shown in Fig. 2.

The total Hamiltonian can be described by ($\hbar = \kappa_B = 1$ throughout this article)

$$H = \sum_{i=1}^4 \omega_i a_i^\dagger a_i + J_1 a_1^\dagger a_2 + J_2 a_1^\dagger a_3 + J_3 a_4^\dagger a_2 + J_x a_4^\dagger a_3 + J_0 a_2^\dagger a_3 + h.c., \quad (3)$$

where a_i (a_i^\dagger) denotes annihilation (creation) operator of the i th cavity mode with the corresponding frequency ω_i ; J_1 , J_2 , J_3 , J_x , J_0 represent the coupling strength between cavity modes 1 and 2, 1 and 3, 2 and 4, 3 and 4, 2 and 3, respectively. The coupling strengths J_1 , J_2 , J_3 , J_0 are known and tunable. The unknown coupling strength J_x is what we want to measure.

The cavity modes 1 and 4 are coupled with two Markovian thermal baths. The whole dynamic can be described by quantum Langevin-Heisenberg equation

$$\dot{\vec{a}} = \mathbf{M}\vec{a} + \vec{a}_{\text{in}} \quad (4)$$

where the cavity mode vector $\vec{a} = (a_1, a_2, a_3, a_4)^\top$, the evolution matrix \mathbf{M} is expressed as

$$\mathbf{M} = \begin{pmatrix} -i\omega_1 - \kappa_1 & -iJ_1 & -iJ_2 & 0 \\ -iJ_1 & -i\omega_2 & -iJ_0 & -iJ_3 \\ -iJ_2 & -iJ_0 & -i\omega_3 & -iJ_x \\ 0 & -iJ_3 & -iJ_x & -i\omega_4 - \kappa_4 \end{pmatrix}.$$

And $\vec{a}_{\text{in}} = (\sqrt{2\kappa_1}a_{1\text{in}}(t), 0, 0, \sqrt{2\kappa_4}a_{4\text{in}}(t))^T$, where the input noise operators $a_{j\text{in}}$ satisfy that

$$\langle a_{j\text{in}}^\dagger(t) \rangle = 0, \quad (5)$$

$$\langle a_{j\text{in}}^\dagger(t)a_{j\text{in}}(t') \rangle = N_j \delta(t - t'), \quad (6)$$

$$\langle a_{j\text{in}}(t')a_{j\text{in}}^\dagger(t) \rangle = (N_j + 1)\delta(t - t'), \quad (7)$$

where the thermal average boson number $N_j = \frac{1}{\exp(\omega_j/T_j) - 1}$ with $j = 1, 4$. κ_j is the coupling strength between the cavity mode j and the thermal bath j with the temperature T_j . $\langle \cdot \rangle$ represents the mean over the state of the bath degrees of freedom.

III. QUANTUM WHEATSTONE BRIDGE BALANCE CRITERION

When $J_x = \frac{J_2}{J_1}J_3$ at the balance point, the Hamiltonian in Eq. (3) can be rewritten with bright mode $A_+ = J_1 a_2 + J_2 a_3$ and dark mode $A_- = J_2 a_2 - J_1 a_3$

$$H = \omega_1 a_1^\dagger a_1 + \omega_4 a_4^\dagger a_4 + \lambda_+ A_+^\dagger A_+ + \lambda_- A_-^\dagger A_- + a_1^\dagger A_+ + J_3/J_1 a_4^\dagger A_+ + h.c., \quad (8)$$

The dark mode A_- decouples with the cavity modes a_1 and a_4 , which are subjected to Markovian thermal baths. In order to make the Hamiltonian in the above equation be equal to the Hamiltonian in Eq. (3). The values of λ_+ and λ_- should satisfy the following conditions

$$\lambda_+ J_1^2 + \lambda_- J_2^2 = \omega_2, \quad (9)$$

$$\lambda_+ J_2^2 + \lambda_- J_1^2 = \omega_3, \quad (10)$$

$$\lambda_+ - \lambda_- = \frac{J_0}{J_1 J_2}. \quad (11)$$

The above equations have a solution only if

$$\omega_3 - \omega_2 = J_0 \left(\frac{J_2}{J_1} - \frac{J_1}{J_2} \right). \quad (12)$$

When Eq. (2) and Eq. (12) hold, we can get the dark mode $A_-(t) = J_2 a_2(t) - J_1 a_3(t)$, i.e.,

$$A_-(t \rightarrow \infty) = e^{i\varphi(t)} A_-(t = 0), \quad (13)$$

where the phase $\varphi(t)$ is real. Based on the existence of the dark mode, we next find the detail balance criterion of quantum Wheatstone bridge.

For $\kappa_1, \kappa_4 \gg |\omega_i - \omega_j|$ with $\{i, j\} = \{1, 2, 3, 4\}$, we can analytically obtain the solution of Eq. (4) (see the detail

in Appendix). The solutions of the modes $a_2(t)$ and $a_3(t)$ can be given by

$$\begin{pmatrix} a_2(t) \\ a_3(t) \end{pmatrix} = e^{\mathbf{M}_2 t} \begin{pmatrix} a_2(0) \\ a_3(0) \end{pmatrix} + \int_0^t e^{\mathbf{M}_2(t-t')} \begin{pmatrix} A_{2\text{in}}(t') \\ A_{3\text{in}}(t') \end{pmatrix} dt', \quad (14)$$

where the evolution matrix \mathbf{M}_2 is described by

$$\mathbf{M}_2 = \begin{pmatrix} -i\omega_2 - \frac{J_1^2}{\kappa_1} - \frac{J_3^2}{\kappa_4} & -iJ_0 - \frac{J_1 J_2}{\kappa_1} - \frac{J_3 J_4}{\kappa_4} \\ -iJ_0 - \frac{J_1 J_2}{\kappa_1} - \frac{J_3 J_4}{\kappa_4} & -i\omega_3 - \frac{J_2^2}{\kappa_1} - \frac{J_4^2}{\kappa_4} \end{pmatrix}, \quad (15)$$

and the noise operators are

$$A_{2\text{in}}(t) = -\sqrt{2}i \left[\frac{J_1 a_{1\text{in}}(t)}{\sqrt{\kappa_1}} + \frac{J_3 a_{4\text{in}}(t)}{\sqrt{\kappa_4}} \right], \quad (16)$$

$$A_{3\text{in}}(t) = -\sqrt{2}i \left[\frac{J_2 a_{1\text{in}}(t)}{\sqrt{\kappa_1}} + \frac{J_4 a_{4\text{in}}(t)}{\sqrt{\kappa_4}} \right]. \quad (17)$$

When $J_1 \neq J_2$ and the quantum Wheatstone bridge is balanced, the eigenvalues of \mathbf{M}_2 can be achieved

$$E_1 = -\frac{i(J_1^2 \omega_2 - J_2^2 \omega_3)}{J_1^2 - J_2^2}, \quad (18)$$

$$E_2 = -\frac{(J_1^2 + J_2^2)(J_3^2 \kappa_1 + J_4^2 \kappa_4)}{J_1^2 \kappa_1 \kappa_4} - \frac{i(J_1^2 \omega_2 - J_2^2 \omega_3)}{J_1^2 - J_2^2}. \quad (19)$$

The eigenvalue E_1 is pure imaginary, which means that $e^{\mathbf{M}_2 t} \neq \mathbf{0}$ for the long time limit $t \rightarrow \infty$. It leads to that the expectations of the cavity modes 2 and 3 are described by

$$\langle a_2(t \rightarrow \infty) \rangle = \frac{e^{E_1 t} J_2}{J_1^2 + J_2^2} \langle J_2 a_2(0) - J_1 a_3(0) \rangle; \quad (20)$$

$$\langle a_3(t \rightarrow \infty) \rangle = \frac{e^{E_1 t} J_1}{J_1^2 + J_2^2} \langle J_1 a_3(0) - J_2 a_2(0) \rangle, \quad (21)$$

where $\langle \star \rangle$ denotes the mean over the initial state of the cavity modes. When $J_x \neq \frac{J_2}{J_1} J_3$, the real parts of the eigenvalues of \mathbf{M}_2 are all negative. As a result, the expectation values $\langle a_2(t \rightarrow \infty) \rangle = \langle a_3(t \rightarrow \infty) \rangle = 0$.

When $J_1 = J_2$, the frequency ω_2 must be equal to ω_3 for achieving the balanced quantum Wheatstone bridge. In this case, the coupling strength J_0 can be arbitrary value, which is different from the case of $J_1 \neq J_2$. The corresponding eigenvalues of \mathbf{M}_2 are

$$E'_1 = i(J_0 - \omega_3), \quad (22)$$

$$E'_2 = i(J_0 - \omega_3) - \frac{2J_1^2}{\kappa_1} - \frac{2J_3^2}{\kappa_4}. \quad (23)$$

For the long time limit $t \rightarrow \infty$, we get the similar form as the previous results

$$\langle a_2(t \rightarrow \infty) \rangle = \frac{e^{E'_1 t}}{2} \langle a_2(0) - a_3(0) \rangle; \quad (24)$$

$$\langle a_3(t \rightarrow \infty) \rangle = \frac{e^{E'_1 t}}{2} \langle a_3(0) - a_2(0) \rangle. \quad (25)$$

From Eq. (18), we can derive that $\lim_{J_1 \rightarrow J_2} E_1 = -i\omega_3$, which is different from E'_1 unless that J_0 is equal to 0. As a result, there is a discontinuity for the phase of $\langle a_2(t \rightarrow \infty) \rangle$ and $\langle a_3(t \rightarrow \infty) \rangle$.

The detail balance criterion of quantum Wheatstone bridge can be summarized as follows: With the initial state of cavity modes 2 and 3 in the coherent state $|\alpha\rangle|0\rangle$, it is balanced when the expectation values of $\langle a_2(t \rightarrow \infty) \rangle$ and $\langle a_3(t \rightarrow \infty) \rangle$ are not equal to 0; otherwise it is not balanced.

IV. LOCAL HOMODYNE DETECTION

By the homodyne detection of the cavity mode $a_2(t \rightarrow \infty)$ or $a_3(t \rightarrow \infty)$, we can obtain the information of J_x . The uncertainty of J_x can be achieved by the error transfer formula

$$\delta J_x = \frac{\sqrt{\langle X^2 \rangle - \langle X \rangle^2}}{\left| \frac{d\langle X \rangle}{dJ_x} \right|}, \quad (26)$$

where X denotes the measurement operator.

A. In the case of $J_1 = J_2$

When $J_1 = J_2$ and $\omega_2 = \omega_3$, we can analytically obtain the differential coefficients

$$\lim_{J_x \rightarrow J_3} \frac{d}{dJ_x} \langle a_2(t \rightarrow \infty) \rangle = \frac{J_3 \kappa_1 e^{it(J_0 - \omega_3)} \langle a_2(0) \rangle}{2(J_3^2 \kappa_1 + J_2^2 \kappa_4 + iJ_0 \kappa_1 \kappa_4)}, \quad (27)$$

$$\lim_{J_x \rightarrow J_3} \frac{d}{dJ_x} \langle a_3(t \rightarrow \infty) \rangle = \frac{-J_3 \kappa_1 e^{it(J_0 - \omega_3)} \langle a_3(0) \rangle}{2(J_3^2 \kappa_1 + J_2^2 \kappa_4 + iJ_0 \kappa_1 \kappa_4)}. \quad (28)$$

For the long evolution time $t > \tau = 1/(\frac{2J_1^2}{\kappa_1} + \frac{2J_3^2}{\kappa_4})$, we can derive the Taylor series expansion

$$\langle a_2(t) \rangle = \frac{1}{2} e^{E'_1 t - \Gamma y^2 t - o(y^3)t} \langle (1 + \Lambda y + o(y^2)) a_2(0) - (1 + o(y^2)) a_3(0) \rangle; \quad (29)$$

$$\langle a_3(t) \rangle = -\frac{1}{2} e^{E'_1 t - \Gamma y^2 t - o(y^3)t} \langle (1 + o(y^2)) a_2(0) - (1 - \Lambda y + o(y^2)) a_3(0) \rangle, \quad (30)$$

where the coefficients $\Gamma = \frac{J_2^2 + iJ_0 \kappa_1}{2(J_3^2 \kappa_1 + J_2^2 \kappa_4 + iJ_0 \kappa_1 \kappa_4)}$, $\Lambda = \frac{J_3 \kappa_1}{J_3^2 \kappa_1 + J_2^2 \kappa_4 + iJ_0 \kappa_1 \kappa_4}$ and the difference $y = J_x - J_3$. For larger difference, $y \geq 1$, the expectation values of $\langle a_2(t) \rangle$ and $\langle a_3(t) \rangle$ go to 0 very quickly. Therefore, we consider that $y < 1$. It leads to that higher-order terms $o(y^3)t$ and $o(y^2)$ can be ignored.

We consider the homodyne detection with the local quadrature operator $X_{\varphi_j} = a_j e^{-i\varphi_j} + a_j^\dagger e^{-i\varphi_j}$, where φ_j

represents phase with $j = 2, 3$. The initial states of cavity 2 and 3 are given by the classical coherent state $|\alpha\rangle_2|0\rangle_3$, with the real value α . By utilizing Eq. (26), we can obtain the measurement precision of J_x with the quadrature operator X_{φ_2}

$$\delta J_x = \frac{\sqrt{1+f}}{|Re[(\Lambda - 2\Gamma y t(1 + \Lambda y))e^{i\varphi_2 + E_1 t - \Gamma y^2 t}]\alpha|}, \quad (31)$$

where the quantum fluctuation $f = \frac{J_1^2 N_1 \kappa_4 + J_3^2 N_4 \kappa_1}{J_1^2 \kappa_4 + J_3^2 \kappa_1}$. From the above equation, one can find that δJ_x takes the minimum value at $y = 0$. It shows that the optimal precision of J_x can be obtained when the Wheatstone bridge is balanced:

$$\delta J_x(y=0) = \frac{\sqrt{1+f}\sqrt{(J_3^2 \kappa_1 + J_2^2 \kappa_4)^2 + J_0^2 \kappa_1^2 \kappa_4^2}}{J_3 \kappa_1 |\cos(\varphi_2 + \theta + (J_0 - \omega_3)t)|\alpha}, \quad (32)$$

where the phase θ satisfies that $e^{i\theta} = \Lambda/|\Lambda|$. When the phase satisfies that $\varphi_2 + \theta + (J_0 - \omega_3)t = n\pi$ (n represents an integer), the optimal precision by the homodyne detection can be expressed as

$$\delta J_x^o = \frac{\sqrt{1+f}\sqrt{(J_3^2 \kappa_1 + J_2^2 \kappa_4)^2 + J_0^2 \kappa_1^2 \kappa_4^2}}{J_3 \kappa_1 \alpha}. \quad (33)$$

Let $J_0 = 0$, the precision can be further improved,

$$\delta J_x^o(J_0 = 0) = \frac{\sqrt{1+f}(J_3^2 \kappa_1 + J_2^2 \kappa_4)}{J_3 \kappa_1 \alpha}. \quad (34)$$

B. In the case of $J_1 \neq J_2$

In the case of $J_1 \neq J_2$, we can get the derivative at the balance point

$$\lim_{J_x \rightarrow J_3} \frac{d}{dJ_x} \langle a_2(t \rightarrow \infty) \rangle = \frac{2J_1^3 J_2 J_3 \kappa_1 e^{E_1 t} \langle a_2(0) \rangle}{\mu} - \frac{(J_1^2 - J_2^2) J_1^2 J_3 \kappa_1 e^{E_1 t} \langle a_3(0) \rangle}{\mu}, \quad (35)$$

$$\lim_{J_x \rightarrow J_3} \frac{d}{dJ_x} \langle a_3(t \rightarrow \infty) \rangle = -\frac{2J_1^3 J_2 J_3 \kappa_1 e^{E_1 t} \langle a_3(0) \rangle}{\mu} - \frac{(J_1^2 - J_2^2) J_1^2 J_3 \kappa_1 e^{E_1 t} \langle a_2(0) \rangle}{\mu}, \quad (36)$$

where $\mu = (J_1^2 + J_2^2)^2 (J_3^2 \kappa_1 + J_1^2 \kappa_4 + iJ_0 J_1 \kappa_1 \kappa_4 / J_2)$. The measurement precision of J_x can be given by

$$\delta J_x = \frac{\sqrt{1+f_c}|\mu|}{4J_1^3 J_2 J_3 \kappa_1 \alpha |\cos(\varphi_2 + \theta' + \frac{J_1^2 \omega_2 - J_2^2 \omega_3}{J_1^2 - J_2^2} t)|}, \quad (37)$$

where the phase θ' satisfies that $e^{i\theta'} = |\mu|/\mu$ and the quantum fluctuation $f_c = \frac{2J_1^2 N_1 \kappa_4 + 2J_3^2 N_4 \kappa_1}{(J_1^2 \kappa_4 + J_3^2 \kappa_1)(J_1^2 + J_2^2)}$. When the phase satisfies that $\varphi_2 + \theta' - iE_1 t = n\pi$, the optimal

precision with the homodyne detection can be expressed as

$$\delta J_x^o = \frac{\sqrt{1+f_c}|\mu|}{4J_1^3 J_2 J_3 \kappa_1 \alpha}. \quad (38)$$

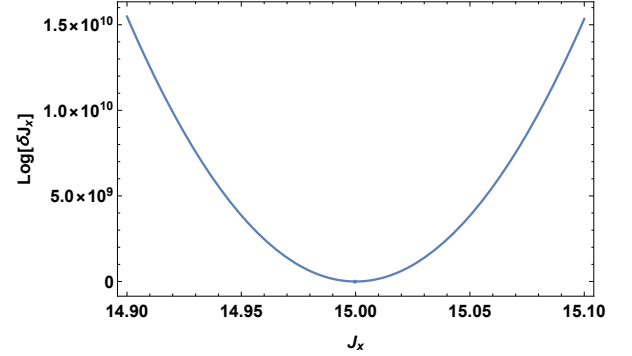


Figure 3. A plot of the logarithm of the uncertainty of J_x versus J_x . Here, the dimensionless parameters are set as: $\omega_2 = 100$, $\omega_3 = 101$, $\alpha = 10000$, $\kappa_1 = 10$, $\kappa_4 = 10$, $J_1 = 10$, $J_2 = 15$, $J_3 = 10$, and $J_0 = (\omega_3 - \omega_2)J_1 J_2 / (J_2^2 - J_1^2) = 1.2$. At the balance point, the unknown coupling strength $J_x = J_2 J_3 / J_1 = 15$.

When $J_1 = J_2$, Eq. (38) becomes Eq. (33). It shows that the optimal precision is still continuous at the point $J_1 = J_2$ and not affected by the discontinuity for the phase of $\langle a_2(t \rightarrow \infty) \rangle$ and $\langle a_3(t \rightarrow \infty) \rangle$. This is mainly because the measurement angle φ_2 can compensate of the effect of phase.

As shown in Fig. 3, we can see that the minimum uncertainty of J_x appears when the quantum Wheatstone bridge is balanced, i.e., $J_x = J_2 J_3 / J_1 = 15$. Consistent with the previous results, the measurement precision at the balance point is optimal.

V. QUANTUM FISHER INFORMATION OF J_x

The quantum Cramér-Rao bound [21–24] provides the bound on the estimation precision of parameter J_x ,

$$\delta J_x \geq \frac{1}{\mathcal{F}[J_x]}, \quad (39)$$

where $\mathcal{F}[J_x]$ denotes the quantum Fisher information of J_x , which is encoded into the cavity modes. Due to that Hamiltonian is quadratic and the initial state is Gaussian, the steady state of cavity modes 2 and 3 is Gaussian too [25]. The Quantum Fisher information for Gaussian state is obtained through the fidelity by Pinel *et al.* in 2013 [26],

$$\mathcal{F}[J_x] = \frac{1}{2(1 + P_{J_x}^2)} \text{Tr}[(C_{J_x}^{-1} C'_{J_x})^2] + \frac{2P_{J_x}^2}{1 - P_{J_x}^4} + \langle \mathbf{X}^\top \rangle'_{J_x} C_{J_x}^{-1} \langle \mathbf{X} \rangle'_{J_x}, \quad (40)$$

where $P_{J_x} = \frac{1}{2d}$, $d = \sqrt{\text{Det } \mathcal{C}_{J_x}}$ and A'_{J_x} is the term by term derivative of A_{J_x} with respect to J_x . The entries of the covariance matrix \mathcal{C} are defined as $\mathcal{C}_{ij} := \frac{1}{2}(\langle \mathbf{X}_i, \mathbf{X}_j \rangle) - \langle \mathbf{X}_i \rangle \langle \mathbf{X}_j \rangle$, with $\langle \bullet \rangle$ the expectation value. The vector of quadrature operators is $\mathbf{X} = (q_2, q_3, p_2, p_3)^\top$, where the quadrature operators are defined as $q_j := (a_j + a_j^\dagger)$ and $p_j := \frac{1}{i}(a_j - a_j^\dagger)$.

By utilizing Eq. (20) and Eq. (21), we can obtain the covariance matrix

$$\mathcal{C} = \begin{pmatrix} 1 + f_c & \frac{f_c J_2}{J_1} & 0 & 0 \\ \frac{f_c J_2}{J_1} & 1 + \frac{f_c J_2^2}{J_1^2} & 0 & 0 \\ 0 & 0 & 1 + f_c & \frac{f_c J_2}{J_1} \\ 0 & 0 & \frac{f_c J_2}{J_1} & 1 + \frac{f_c J_2^2}{J_1^2} \end{pmatrix}. \quad (41)$$

And using Eq. (35) and Eq. (36), the derivative of the vector of quadrature operators is given by

$$\langle \mathbf{X} \rangle'_{J_x} = \frac{\alpha J_1^2 J_3 \kappa_1}{|\mu|} (4J_1 J_2 \cos \phi, 2(J_2^2 - J_1^2) \cos \phi, 4J_1 J_2 \sin \phi, 2(J_2^2 - J_1^2) \sin \phi), \quad (42)$$

where $\phi = \theta' - iE_1 t$.

When the input probes are sufficiently strong, the quantum Fisher information can be dominated by the last term in Eq. (40)[27]

$$\mathcal{F}[J_x] \approx \langle \mathbf{X}^\top \rangle'_{J_x} \mathcal{C}_{J_x}^{-1} \langle \mathbf{X} \rangle'_{J_x} \quad (43)$$

$$= \frac{(\alpha J_1^2 J_3 \kappa_1)^2}{|\mu|^2} \frac{4(1 + f_c) J_1^2 (J_1^2 + J_2^2)^2}{(1 + f_c) J_1^2 + f_c J_2^2} \quad (44)$$

According to the quantum Cramér-Rao bound, the uncertainty of J_x is

$$\delta J_x \geq \frac{g \sqrt{1 + f_c} |\mu|}{4 J_1^3 J_2 J_3 \kappa_1 \alpha}, \quad (45)$$

where the coefficient $g = \frac{2J_2 \sqrt{(1+f_c)J_1^2 + f_c J_2^2}}{(J_1^2 + J_2^2)(1+f_c)}$.

By a simple calculation, we can prove that

$$1 - g^2 = \frac{[(1 + f_c)J_1^2 + (f_c - 1)J_2^2]^2}{(J_1^2 + J_2^2)^2(1 + f_c)^2} \geq 0. \quad (46)$$

It means that the coefficient $g \leq 1$. When $J_2^2 = \frac{1+f_c}{1-f_c} J_1^2$, the equality holds, i.e., $g = 1$. Comparing with Eq. (38), it shows that the homodyne detection is the optimal measurement in the case of $J_2^2 = \frac{1+f_c}{1-f_c} J_1^2$ and $\alpha \gg 1$. In order to get the equation $J_2^2 = \frac{1+f_c}{1-f_c} J_1^2$, the quantum fluctuation f_c must be less than 1. It means that the temperature of both thermal baths should be relatively small. When $f_c = 0$, i.e., the temperature of both thermal baths is 0 ($T_1 = T_4 = 0$)

$$\delta J_x \geq \frac{|\mu|}{2 J_1^3 J_3 \kappa_1 (J_1^2 + J_2^2) \alpha}. \quad (47)$$

For large quantum fluctuation $f_c > 1$, the homodyne detection is not the optimal measurement. With the homodyne detection, the precision of J_x decreases as the quantum fluctuation term f_c increases. With the optimal measurement, the precision of J_x becomes increasingly independent of the quantum fluctuation term f_c . For $f_c \gg 1$, the precision of J_x is given by

$$\delta J_x \geq \frac{|\mu|}{2 J_1^3 J_3 \kappa_1 \sqrt{J_1^2 + J_2^2} \alpha}. \quad (48)$$

Especially, in the case of $J_1 = J_2$, $\omega_2 = \omega_3$ and $J_0 = 0$, the optimal measurement precision of J_x is given by

$$\delta J_x^o = \frac{\sqrt{1 + 2f} (J_3^2 \kappa_1 + J_2^2 \kappa_4)}{J_3 \kappa_1 \alpha \sqrt{1 + f}}. \quad (49)$$

From the above equation, we can see that the measurement uncertainty of J_x increases with the quantum fluctuation f_c . And the ratio $\delta J_x(f_c = 0)/\delta J_x(f_c \rightarrow \infty) = 1/\sqrt{2}$. It shows that quantum fluctuations can reduce the precision by up to a factor of $1/\sqrt{2}$. However, the uncertainty with the local homodyne detection still increases. Hence, it is necessary to construct an optimal nonlocal measurement operator to reduce the influence of the quantum fluctuation.

VI. DISSIPATION OF CAVITY 2 AND 3

When the cavity modes 2 and 3 are not perfect, there are intrinsic losses. This will prevent us from determining whether quantum Wheatstone bridge is balanced. This can be overcome by using gains to make up for losses. The gain process can be achieved by coupling with an amplifying channel [27] or harnessing the feeding fields [28, 29].

Including the intrinsic losses and the gains, quantum Langevin-Heisenberg equation of the cavity modes 2 and 3 can be described as

$$\begin{aligned} \dot{a}_2 = & -iJ_1 a_1 + (-i\omega_2 - \kappa_2 + \gamma_2) a_2 - iJ_0 a_3 - iJ_3 a_4 + \\ & \sqrt{2k_2} a_{2\text{in}}(t) - \sqrt{2\gamma_2} d_{2\text{in}}^\dagger(t); \end{aligned} \quad (50)$$

$$\begin{aligned} \dot{a}_3 = & -iJ_2 a_1 - iJ_0 a_2 + (-i\omega_3 - \kappa_3 + \gamma_3) a_3 - iJ_x a_4 + \\ & \sqrt{2k_3} a_{3\text{in}}(t) - \sqrt{2\gamma_3} d_{3\text{in}}^\dagger(t); \end{aligned} \quad (51)$$

where κ_2, κ_3 are the intrinsic loss rates of the cavity modes 2, 3, respectively; γ_2, γ_3 are the gain rates of the cavity modes 2,3 respectively; the noise operator $Y_{\text{jin}}(t)$ satisfies

$$\langle Y_{\text{jin}}^\dagger(t) \rangle = 0, \quad (52)$$

$$\langle Y_{\text{jin}}^\dagger(t) Y_{\text{jin}}(t') \rangle = 0, \quad (53)$$

$$\langle Y_{\text{jin}}(t') Y_{\text{jin}}^\dagger(t) \rangle = \delta(t - t'), \quad (54)$$

where $Y = a, d$ and $j = 2, 3$.

Let the gain rate γ_j be equal to the corresponding loss rate κ_j ($\kappa_j = \gamma_j$), the quantum Wheatstone bridge balance criterion is reestablished. In the case of $\kappa_j = \gamma_j$, the solution can be obtained

$$\begin{pmatrix} a_2(t) \\ a_3(t) \end{pmatrix} = e^{\mathbf{M}_2 t} \begin{pmatrix} a_2(0) \\ a_3(0) \end{pmatrix} + \int_0^t e^{\mathbf{M}_2(t-t')} \begin{pmatrix} A_{2in}(t') \\ A_{3in}(t') \end{pmatrix} dt', \quad (55)$$

where the noise operators are redefined as

$$A_{2in}(t) = -\sqrt{2}i \left[\frac{J_1 a_{1in}(t)}{\sqrt{\kappa_1}} + \frac{J_3 a_{4in}(t)}{\sqrt{\kappa_4}} \right] + \sqrt{2k_2} (a_{2in}(t) - d_{2in}^\dagger(t)), \quad (56)$$

$$A_{3in}(t) = -\sqrt{2}i \left[\frac{J_2 a_{1in}(t)}{\sqrt{\kappa_1}} + \frac{J_x a_{4in}(t)}{\sqrt{\kappa_4}} \right] + \sqrt{2k_3} (a_{3in}(t) - d_{3in}^\dagger(t)). \quad (57)$$

For simplicity, we assume $\kappa_2 = \kappa_3$. As a result, the optimal measurement precision can be described as

$$\delta J_x \geq \frac{g\sqrt{1+f_c'}|\mu|}{4J_1^3 J_2 J_3 \kappa_1 \alpha}, \quad (58)$$

where the quantum fluctuation $f_c' = f_c + \frac{\kappa_1 \kappa_2 \kappa_4}{2(J_1^2 \kappa_4 + J_2^2 \kappa_1)}$. The increment of quantum fluctuation $f_c' - f_c$ is from the dissipation and the gain environment of the cavity modes 2 and 3. The gain can compensate for the dissipation and reach the balanced quantum Wheatstone bridge, but it can not completely eliminate the effect of quantum fluctuation from the dissipative cavity modes 2 and 3 on the estimation precision. For the quantum fluctuation $f_c \gg 1$, the estimation precision is independent of f_c . In this case, the dissipation and the gain environment of the cavity modes 2 and 3 do not result in a loss of the estimation precision.

VII. POSSIBLE EXPERIMENTAL IMPLEMENTATIONS

Our model with $J_0 = 0$ can be realized in the optomechanical system. Let the cavity modes 2 and 3 become two mechanical modes. The total Hamiltonian can be rewritten as

$$H_{\text{om}} = \sum_{i=1}^4 \omega_i a_i^\dagger a_i + G_1 a_1^\dagger a_1 (a_2 + a_2^\dagger) + G_2 a_1^\dagger a_1 (a_3 + a_3^\dagger) + G_3 a_4^\dagger a_4 (a_2 + a_2^\dagger) + G_x a_4^\dagger a_4 (a_3 + a_3^\dagger), \quad (59)$$

where a_2 and a_3 represent the bosonic annihilation operators of the mechanical modes. Replacing the cavity modes with the sum of its quantum fluctuation operator classical mean value, the Hamiltonian can be linearized in the interaction picture as [30]

$$H_{\text{om,int}} = J_1 a_1^\dagger a_2 + J_2 a_1^\dagger a_3 + J_3 a_4^\dagger a_2 + J_x a_4^\dagger a_3 + h.c., \quad (60)$$

where $J_i = G_i \beta_i$ is the effective optomechanical coupling strength and classical amplitude β_i can be controlled by the classical driving with $i = (1, 2, 3, x)$.

In experiment, this setup has been created by a superconducting circuit of aluminum on a sapphire substrate [31], the microchip circulator device composed of three high-impedance spiral inductors capacitively coupled to the in-plane vibrational modes of a dielectric nanostring mechanical resonator [32]. Therefore, our proposed scheme can be implemented using current experimental technology.

VIII. CONCLUSION

We utilized Bose system to construct the general quantum Wheatstone bridge. We propose a more feasible criterion for determining the balance of the quantum Wheatstone bridge. By calculating the quantum Fisher information, we show that the local homodyne detection is close to the optimal measurement with low temperature of the Markovian baths. With the optimal measurement, the measurement precision of the unknown coupling strength is independent of the quantum fluctuation from the baths with high temperature. In order to maintain the balance criterion of the quantum Wheatstone bridge, extra gain process is proposed to resist the dissipation. Our proposed scheme can be realized in the current optomechanical systems, which will facilitate the precision measurement of photomechanical coupling strength.

ACKNOWLEDGEMENTS

This research was supported by the National Natural Science Foundation of China (Grant No. 62001134), Guangxi Natural Science Foundation (Grant No. 2020GXNSFAA159047, 2020GXNSFAA159007), and National Key R&D Program of China (Grant No. 2018YFB1601402-2).

APPENDIX A

Using the slowly varying operators $S_i = a_i e^{i\omega_i t}$, the Eq.(A2) can be rewritten as

$$\dot{\vec{S}} = \mathbf{M}\vec{S} + \vec{a}_{in} \quad (A1)$$

where $\vec{a}_{in} = (e^{i\omega_1 t} \sqrt{2\kappa_1} a_{1in}(t), 0, 0, e^{i\omega_4 t} \sqrt{2\kappa_4} a_{4in}(t))^T$, and the evolution matrix \mathbf{M} is expressed as

$$\mathbf{M}' = \begin{pmatrix} -\kappa_1 & -iJ_1' & -iJ_2' & 0 \\ -iJ_1'^* & 0 & -iJ_0' & -iJ_3' \\ -iJ_2'^* & -iJ_0'^* & 0 & -iJ_x' \\ 0 & -iJ_3'^* & -iJ_x'^* & -\kappa_4 \end{pmatrix}, \quad (A2)$$

where $J'_1 = J_1 e^{-i\Delta_{21}t}$, $J'_2 = J_2 e^{-i\Delta_{31}t}$, $J'_3 = J_3 e^{-i\Delta_{42}t}$, $J'_x = J_x e^{-i\Delta_{43}t}$ and $J'_0 = J_0 e^{-i\Delta_{32}t}$ with the frequency detunings between two cavity modes $\Delta_{ij} = \omega_i - \omega_j$.

We can obtain the formal solutions of S_1 and S_4

$$S_1 = -i \int_0^t dt' e^{-\kappa_1(t-t')} [J'_1 S_2(t') + J'_2 S_3(t')] + \int_0^t dt' e^{-\kappa_1(t-t')} [\sqrt{2\kappa_1} a'_{1in}(t')]; \quad (\text{A3})$$

$$S_4 = -i \int_0^t dt' e^{-\kappa_4(t-t')} [J'^*_3 S_2(t') + J'^*_x S_3(t')] + \int_0^t dt' e^{-\kappa_4(t-t')} [\sqrt{2\kappa_4} a'_{4in}(t')]. \quad (\text{A4})$$

We consider that the dissipation rates of the cavity modes a_1 and a_4 is much larger than the cases of the cavity modes a_2 and a_3 , i.e., $\kappa_1, \kappa_4 \gg \kappa_2, \kappa_3$, where we assume that the dissipation rates of the cavity modes a_2 and a_3 : $\kappa_2 = 0, \kappa_3 = 0$ for simplicity. The changes of mode S_2 and S_3 are small within the range of the integration of the cavity modes S_1 and S_4 . Therefore, we can set $S_2(t') = S_2(t)$ and $S_3(t') = S_3(t)$ in Eq. (A3) and Eq. (A4) to obtain

$$S_1 = \frac{-iJ_1 S_2}{\kappa_1 - i\Delta_{21}} e^{-i\Delta_{21}t} + \frac{-iJ_2 S_3}{\kappa_1 - i\Delta_{31}} e^{-i\Delta_{31}t} + \frac{\sqrt{2\kappa_1} a_{1in}}{\kappa_1} e^{-i\omega_1 t}; \quad (\text{A5})$$

$$S_4 = \frac{-iJ_3 S_2}{\kappa_4 - i\Delta_{24}} e^{-i\Delta_{24}t} + \frac{-iJ_x S_3}{\kappa_4 - i\Delta_{34}} e^{-i\Delta_{34}t} + \frac{\sqrt{2\kappa_4} a_{4in}}{\kappa_4} e^{-i\omega_4 t}. \quad (\text{A6})$$

Substituting the above equations into Eq. (A1), the modes S_1 and S_4 can be adiabatically eliminated. The corresponding evolution equations of the modes S_2 and

S_3 are reduced to

$$\dot{S}_2 = \left(-\frac{J_1^2}{\kappa_1 - i\Delta_{21}} - \frac{J_3^2}{\kappa_1 - i\Delta_{24}} \right) S_2 + \left(-\frac{J_1 J_2}{\kappa_1 - i\Delta_{31}} - \frac{J_3 J_x}{\kappa_4 - i\Delta_{34}} - iJ_0 \right) e^{-i\Delta_{32}t} S_3 - \left(\frac{J_1 a_{1in}}{\sqrt{\kappa_1}} + \frac{J_3 a_{4in}}{\sqrt{\kappa_4}} \right) \sqrt{2} i e^{-i\omega_2 t}; \quad (\text{A7})$$

$$\dot{S}_3 = \left(-\frac{J_1 J_2}{\kappa_1 - i\Delta_{21}} - \frac{J_3 J_x}{\kappa_1 - i\Delta_{24}} - iJ_0 \right) e^{-i\Delta_{23}t} S_2 + \left(\frac{J_2^2}{\kappa_1 - i\Delta_{31}} - \frac{J_x^2}{\kappa_4 - i\Delta_{34}} \right) S_3 - \left(\frac{J_2 a_{1in}}{\sqrt{\kappa_1}} + \frac{J_x a_{4in}}{\sqrt{\kappa_4}} \right) \sqrt{2} i e^{-i\omega_3 t}. \quad (\text{A8})$$

For $\kappa_1, \kappa_4 \gg \Delta_{ij}$, combine these equations with $S_2 = a_2 e^{i\omega_2 t}$ and $S_3 = a_3 e^{i\omega_3 t}$, we can obtain

$$\begin{pmatrix} \dot{a}_2(t) \\ \dot{a}_3(t) \end{pmatrix} = \mathbf{M}_2 \begin{pmatrix} a_2(t) \\ a_3(t) \end{pmatrix} + \begin{pmatrix} A_{2in}(t) \\ A_{3in}(t) \end{pmatrix}, \quad (\text{A9})$$

where the evolution matrix \mathbf{M}_2 is described by

$$\mathbf{M}_2 = \begin{pmatrix} -i\omega_2 - \frac{J_1^2}{\kappa_1} - \frac{J_3^2}{\kappa_4} & -iJ_0 - \frac{J_1 J_2}{\kappa_1} - \frac{J_3 J_x}{\kappa_4} \\ -iJ_0 - \frac{J_1 J_2}{\kappa_1} - \frac{J_3 J_x}{\kappa_4} & -i\omega_3 - \frac{J_2^2}{\kappa_1} - \frac{J_x^2}{\kappa_4} \end{pmatrix}, \quad (\text{A10})$$

and the noise operators are

$$A_{2in}(t) = -\sqrt{2}i \left[\frac{J_1 a_{1in}(t)}{\sqrt{\kappa_1}} + \frac{J_3 a_{4in}(t)}{\sqrt{\kappa_4}} \right], \quad (\text{A11})$$

$$A_{3in}(t) = -\sqrt{2}i \left[\frac{J_2 a_{1in}(t)}{\sqrt{\kappa_1}} + \frac{J_x a_{4in}(t)}{\sqrt{\kappa_4}} \right]. \quad (\text{A12})$$

The solutions of the modes $a_2(t)$ and $a_3(t)$ can be obtained

$$\begin{pmatrix} a_2(t) \\ a_3(t) \end{pmatrix} = e^{\mathbf{M}_2 t} \begin{pmatrix} a_2(0) \\ a_3(0) \end{pmatrix} + \int_0^t e^{\mathbf{M}_2(t-t')} \begin{pmatrix} A_{2in}(t') \\ A_{3in}(t') \end{pmatrix} dt'. \quad (\text{A13})$$

-
- [1] El Mehdi Boujamaa, Yannick Soulie, Frédéric Mailly, Laurent Latorre, Pascal Nouet, Rejection of Power Supply Noise in Wheatstone Bridges : Application to Piezoresistive MEMS, Dans Symposium on Design, Test, Integration and Packaging of MEMS/MOEMS - DTIP 2008, Nice : France (2008).
 - [2] E. Halvorsen, S. Husa, Bridge configurations in piezoresistive two-axis accelerometers, Dans Symposium on Design, Test, Integration and Packaging of MEMS/MOEMS - DTIP 2007, Stresa, lago Maggiore : Italie (2007).
 - [3] S. H. Mennema, J. H. T. Ransley, G. Burnell, J. L. MacManus-Driscoll, E. J. Tarte, and M. G. Blamire, Normal-state properties of high-angle grain boundaries

- in (Y, Ca)Ba₂Cu₃O_{7- δ} , Phys. Rev. B 71, 094509 (2005).
- [4] S. H. Christie, The bakerian lecture: Experimental determination of the laws of magneto-electric induction in different masses of the same metal, and of its intensity in different metals, Philos. T. R. Soc. Lond. 123, 95 (1833)
- [5] C. Wheatstone, Xiii. the bakerian lecture. 2014; an account of several new instruments and processes for determining the constants of a voltaic circuit, Philos. T. R. Soc. Lond. 133, 303 (1843).
- [6] Giovannetti, S. Lloyd, L. Maccone, Quantum-Enhanced measurements: beating the standard quantum limit, Science 306, 1330 (2004).
- [7] Luca Razzoli, Luca Ghirardi, Ilaria Siloi, Paolo Bordone,

- and Matteo G. A. Paris, Lattice quantum magnetometry, *Phys. Rev. A* 99, 062330 (2019)
- [8] Kejie Fang, Victor M. Acosta, Charles Santori, Zhihong Huang, Kohei M. Itoh, Hideyuki Watanabe, Shinichi Shikata, and Raymond G. Beausoleil, High-Sensitivity Magnetometry Based on Quantum Beats in Diamond Nitrogen-Vacancy Centers, *Phys. Rev. Lett.* 110, 130802 (2013).
- [9] Squeezed-Light Optical Magnetometry Florian Wolfgang, Alessandro Cerè, Federica A. Beduini, Ana Predojević, Marco Koschorreck, and Morgan W. Mitchell *Phys. Rev. Lett.* 105, 053601 (2010).
- [10] M. T. Mitchison, T. Fogarty, G. Guarnieri, S. Campbell, T. Busch, and J. Goold, In Situ Thermometry of a Cold Fermi gas via Dephasing Impurities, *Phys. Rev. Lett.* 125, 080402 (2020).
- [11] D. Xie, F. Sun, and C. Xu, Quantum thermometry based on a cavity-QED setup, *Phys. Rev. A* 101, 063844 (2020).
- [12] M. Mehboudi, A. Sanpera, and L. A. Correa, Thermometry in the quantum regime: Recent theoretical progress, *J. Phys. A: Math. Theor.* 52, 303001 (2019).
- [13] S. Campbell, M. Mehboudi, G. D. Chiara, and M. Paternostro, Global and local thermometry schemes in coupled quantum systems, *New J. Phys.* 19, 103003 (2017).
- [14] A. H. Kiilerich, A. De Pasquale, and V. Giovannetti, Dynamical approach to ancilla-assisted quantum thermometry, *Phys. Rev. A* 98, 042124 (2018).
- [15] L. A. Correa, M. Mehboudi, G. Adesso, and A. Sanpera, Individual Quantum Probes for Optimal Thermometry, *Phys. Rev. Lett.* 114, 220405 (2015).
- [16] D. Lang, and Carlton M. Caves, Optimal quantum-enhanced interferometry Matthias, *Phys. Rev. A* 90, 025802 (2014).
- [17] Su-Yong Lee, Yong Sup Ihn, and Zaeill Kim, Quantum illumination via quantum-enhanced sensing, *Phys. Rev. A* 103, 012411 (2021).
- [18] M. Sanz, U. Las Heras, J.J.García-Ripoll, E. Solano, and R. Di Candia, Quantum Estimation Methods for Quantum Illumination, *Phys. Rev. Lett.* 118, 070803 (2017).
- [19] Si-Hui Tan, Baris I. Erkmen, Vittorio Giovannetti, Saikat Guha, Seth Lloyd, Lorenzo Maccone, Stefano Pirandola, and Jeffrey H. Shapiro, Quantum Illumination with Gaussian States, *Phys. Rev. Lett.* 101, 253601 (2008).
- [20] Kasper Poulsen, Alan C. Santos, and Nikolaj T. Zinner, Quantum Wheatstone Bridge, *Phys. Rev. Lett.* 128, 240401 (2022).
- [21] Samuel L. Braunstein, Carlton M. Caves G. J. Milburn, Generalized Uncertainty Relations: Theory, Examples, and Lorentz Invariance, *Ann. Phys. (NY)* 247, 135 (1996).
- [22] Samuel L. Braunstein and Carlton M. Caves, Statistical distance and the geometry of quantum states, *Phys. Rev. Lett.* 72, 3439 (1994).
- [23] H. Cramér, *Mathematical Methods of Statistics* (Princeton University Press, Princeton, 1999).
- [24] C. R. Rao, *Breakthroughs in Statistics* (Springer, New York, 1992).
- [25] Christian Weedbrook, Stefano Pirandola, Ral Garca-Patrón, Nicolas J. Cerf, Timothy C. Ralph, Jeffrey H. Shapiro, and Seth Lloyd, *Rev. Mod. Phys.* 84, 621 (2012).
- [26] O. Pinel, P. Jian, N. Treps, C. Fabre, and D. Braun, Quantum parameter estimation using general single-mode Gaussian states, *Phys. Rev. A* 88, 040102(R) (2013).
- [27] Mengzhen Zhang, William Sweeney, Chia Wei Hsu, Lan Yang, A. D. Stone, and Liang Jiang, Quantum Noise Theory of Exceptional Point Amplifying Sensors, *Phys. Rev. Lett.* 123, 180501 (2019).
- [28] D. Zhang, X. Q. Luo, Y. P. Wang, T. F. Li, and J. Q. You, Observation of the exceptional point in cavity magnon polaritons, *Nat. Commun.* 8, 1368 (2017).
- [29] Y. Sun, W. Tan, H. Q. Li, J. Li, and H. Chen, Experimental Demonstration of a Coherent Perfect Absorber with PT Phase Transition, *Phys. Rev. Lett.* 112, 143903 (2014).
- [30] X.-W. Xu, Y. Li, A.-X. Chen, and Y.-X. Liu, Nonreciprocal Conversion between Microwave and Optical Photons in Electro-Optomechanical Systems, *Phys. Rev. A* 93, 023827 (2016).
- [31] G. A. Peterson, F. Lecocq, K. Cicak, R. W. Simmonds, J. Aumentado, and J. D. Teufel, Demonstration of Efficient Nonreciprocity in a Microwave Optomechanical Circuit, *Phys. Rev. X* 7, 031001 (2017).
- [32] S. Barzanjeh, M. Wulf, M. Peruzzo, M. Kalaei, P.B. Dieterle, O. Painter, and J. M. Fink, Mechanical on-chip microwave circulator, *Nat Commun* 8, 953 (2017).